ISBN: 978-3-95450-184-7 doi:10.18429/JACoW-IPAC2018-WEPAL013

DESIGN OF THE DIAGNOSTIC STATIONS FOR THE ELI-NP COMPTON GAMMA SOURCE

M. Marongiu*[1], A. Mostacci[1], L. Palumbo[1], Sapienza University, Rome, Italy
M. Castellano, E. Chiadroni, G. Di Pirro, G. Franzini, A. Giribono, V.Shpakov, A. Stella, A. Variola, LNF-INFN, Frascati, Italy
A. Cianchi, Università di Roma II Tor Vergata, Rome, Italy
[1]also at INFN, Rome, Italy

Abstract

A high brightness electron Linac is being built in the Compton Gamma Source at the ELI Nuclear Physics facility in Romania. To achieve the design luminosity, a train of 32 bunches, 16 ns spaced, with a nominal charge of 250 pC will collide with the laser beam in the interaction point. Electron beam spot size is measured with optical transition radiation (OTR) profile monitors.

Furthermore, OTR angular distribution strongly depends on beam energy. Since OTR screens are typically placed in several positions along the Linac to monitor beam envelope, one may perform a distributed energy measurement along the machine. This will be useful, for instance, during the commissioning phase of the GBS in order to verify the correct functionality of the C-Band accelerating structures, due to the fact that there are OTR screens after each accelerating module.

This paper deals with the studies of different optic configurations to achieve the field of view, resolution and accuracy in order to measure the energy of the beam. Several configurations of the optical detection line will be studied with simulation tools (e.g. Zemax).

INTRODUCTION

The Gamma Beam Source [1] (GBS) machine is an advanced source of up to ≈20 MeV Gamma Rays based on Compton back-scattering, i.e. collision of an intense high power laser beam and a high brightness electron beam with maximum kinetic energy of about 740 MeV. The Linac will provide trains of bunches in each RF pulse, spaced by the same time interval needed to recirculate the laser pulse in a properly conceived and designed laser recirculator, in such a way that the same laser pulse will collide with all the electron bunches in the RF pulse, before being dumped. The final optimization foresees trains of 32 electron bunches separated by 16 ns, distributed along a 0.5 µs RF pulse, with a repetition rate of 100 Hz.

The goal of this paper is the characterization of different lenses in terms of resolution and magnification for the optical diagnostics for the ELI-NP-GBS LINAC in order to perform a distributed energy measurement by means of Optical Transition Radiation (OTR). The optical diagnostics systems in ELI-NP-GBS will provide an interceptive method to measure beam spot size in different positions along the LINAC.

In a typical monitor setup, the beam is imaged via OTR or YAG screen using standard lens optics, and the recorded intensity profile is a measure of the particle beam spot [2]. In conjunction with other accelerator components, it will also be possible to perform various measurements on the beam, namely: its energy and energy spread (with a dipole or corrector magnet), bunch length [3] (with a RF deflector), Twiss parameters [4] (by means of quadrupole scan) or in general 6D characterization on bunch phase space [5]. Such technique is common in conventional [6] and unconventional [7, 8] high brightness LINACs.

The expected beam energy along the LINAC, provided by preliminary beam dynamics simulation, will vary in the 5 MeV - 320 MeV range [9] for the low energy line.

The optical acquisition system is constituted by a “Hamamatsu Orca-Flash4” [10] for the energy measurement.

TRANSITION RADIATION

Optical Transition Radiation screens are widely used for beam profile measurements, as well as in ELI-GBS [11, 12]. The radiation is emitted when a charged particle beam crosses the boundary between two media with different optical properties. For beam diagnostic purposes the visible part of the radiation is used; an observation geometry in backward direction is chosen corresponding to the reflection of virtual photons at the screen which acts as a mirror.

The main advantages of OTR are the instantaneous emission process allowing fast single shot measurements, and the good linearity (if coherent effects can be neglected). The disadvantages are that the process of radiation generation is invasive, and that the radiation intensity is much lower in comparison to scintillation screens. Another advantage of the OTR is the possibility to measure the beam energy by means of observation of its angular distribution; this technique has been proved feasible by many authors [13, 14]. The angular distribution can be expressed by the well known formula [13]:

$$\frac{dI^2}{d\omega d\Omega} = \frac{e^2}{4\pi^3 c\epsilon_0} \frac{\sin^2\theta}{\left(\frac{1}{\gamma^2} + \sin^2\theta\right)^2} R(\omega, \theta), \qquad (1)$$

where ω is the frequency, Ω is the solid angle, I is the intensity of the radiation, e is the electron charge, c is the speed of light, ϵ_0 is the vacuum permittivity and $R(\omega, \theta)$

* marco.marongiu@uniroma1.it

ISBN: 978-3-95450-184-7 doi:10.18429/JACoW-IPAC2018-WEPAL013

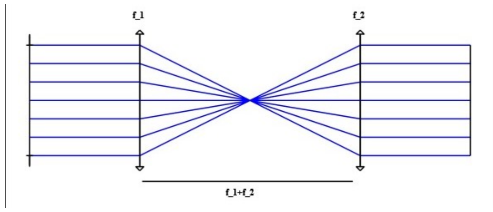

Figure 1: Sketch of the proposed layout based on relay optics. The appropriate choice of the focal lengths f_1 and f_2 allows to obtain any angular magnification and, therefore, obtain the same horizontal resolution on the CCD camera.

is the reflectivity of the screen; the peak of intensity is at $\theta = 1/\gamma$ with respect to the beam direction.

Due to the beam divergence, the angular distribution of the whole beam will be different from 0 at the center: assuming a Gaussian distribution of the divergences, the OTR angular distribution can be written as the convolution between Eq. (1) and the Gaussian distribution as in Eq. (2).

$$
\begin{aligned}
I &\propto \frac{\sqrt{\pi}\mu}{\nu}\Re\left[\Phi(z)\left(\frac{1}{2}+\mu\nu z\right)\right]-\mu^2,\\
\mu &= \frac{1}{\sqrt{2}\sigma'}, \quad \Phi(z) = \frac{1-\mathrm{erf}\,(z)}{\exp\left[-z^2\right]},\\
z &= \mu(\nu + i\theta), \quad \nu = \frac{1}{\gamma}, \qquad (2)
\end{aligned}
$$

where $\mathrm{erf}(z)$ is the complex error function and $\Re$ is the real part [15].

Since for bigger energies the angular distribution narrows, the sensitivity to angular spread is higher than for low energy beams where the angular distribution is wide. Moreover, the beam energy has an effect on the ability of a given optic system to resolve the angular distribution, since the angular distribution narrows as the energy increases; therefore, a change of the optic system (i.e. a bigger focal length) could be necessary.

ZEMAX SIMULATION

ZEMAX [16] is a widely used software in the optics industry as a standard design tool. It is typically used for lens design and illumination devices. The software provides two main analysis modes: the geometrical ray tracing and the physical optics propagation (POP) mode. The former is useful to simulate the behavior of an optical system in the ray approximation, by neglecting any diffraction effects related to the wave nature of the light; however, in order to take into account diffraction effects and polarization, the POP mode is mandatory. This mode, using diffraction laws, propagates a wave front through an optical system surface by surface; the wave front is modeled at every surface using an array of discretely sampled points, each of them storing complex amplitude information about the photon beam. The entire array is then propagated in free space between optical surfaces. At each optical surface, a transfer function is computed which propagates the beam from one side of the optical surface to the other. To propagate the field from one surface to the other, either Fresnel diffraction propagation or an angular spectrum propagation algorithm is used. ZEMAX automatically chooses the algorithm that yields the highest numerical accuracy. Any source of light can be provided in POP mode: the user has to define the spatial distribution of the complex electric field of the source either in a beam file or in a Windows dynamic link library (DLL).

One has to input to ZEMAX the approximation of the electric field for the OTR induced by a single electron (SPF) on a target surface [17]:

$$
\begin{aligned}
E_h &= \frac{e^2}{4\pi^3\epsilon_0 c}\left[\frac{2\pi}{\gamma\lambda}K_1\left(\frac{2\pi}{\gamma\lambda}r\right)-\frac{J_0\left(\frac{2\pi}{\lambda}r\right)}{r}\right]\cos(\phi)\\
E_v &= \frac{e^2}{4\pi^3\epsilon_0 c}\left[\frac{2\pi}{\gamma\lambda}K_1\left(\frac{2\pi}{\gamma\lambda}r\right)-\frac{J_0\left(\frac{2\pi}{\lambda}r\right)}{r}\right]\sin(\phi) \qquad (3)\\
r &= \sqrt{(x-x_0)^2+(y-y_0)^2}\\
\phi &= \arctan\left(\frac{y-y_0}{x-x_0}\right)
\end{aligned}
$$

with $x - x_0$ and $y - y_0$ the two orthogonal coordinates of the target surface measured from the point of electron incidence (x_0, y_0), γ is the relativistic Lorentz factor, λ is the radiation wavelength, K_1 is the modified Bessel function of first order, and J_0 is the Bessel function of zeroth order. The "h,v" indexes represent the horizontal and vertical polarization respectively.

If one wants to perform a distributed energy measurement, he needs to take into consideration the required field of view and resolution at the different beam energies: at low energies, since the angular distribution is wide, one has to put the optics close to the source in order to view the radiation in the camera. At high energy, instead, the angular distribution is narrow: in order to resolve the minimum and the two maxima of the distribution, one needs to let the radiation propagates for a long drift before collect it with the optic system. However, having the camera too close to a source of radiation may damage the camera itself; on the other hand, a long free space propagation may not be feasible due to geometric constraints on the machine or a loss of intensity radiation (and therefore vertical resolution).

A solution could be a relay optics system (see Figure 1): with this system, with an appropriate choice of the focal length and the relative distances, the source is replicated and magnified at a distance that fits the machine constraints. Typically, one wants to acquire the distribution in the range $\theta \in [-4/\gamma : 4/\gamma]$ in order to have enough points between the two maxima and cut the parts of the tails that are affected by the noise (for instance, for a CCD with 2048x2048 pixels of 6.5 µm each like the "Hamamatsu Orca-Flash4" [10], this means to have about 460 pixels between the two maxima). If one call L, the distance between the last lens and the CCD and x_M the position of the maximum of the distribution, one can easily find that $x_M = f_1(L - f_2)/(f_2\gamma)$: for instance,

ISBN: 978-3-95450-184-7 doi:10.18429/JACoW-IPAC2018-WEPAL013

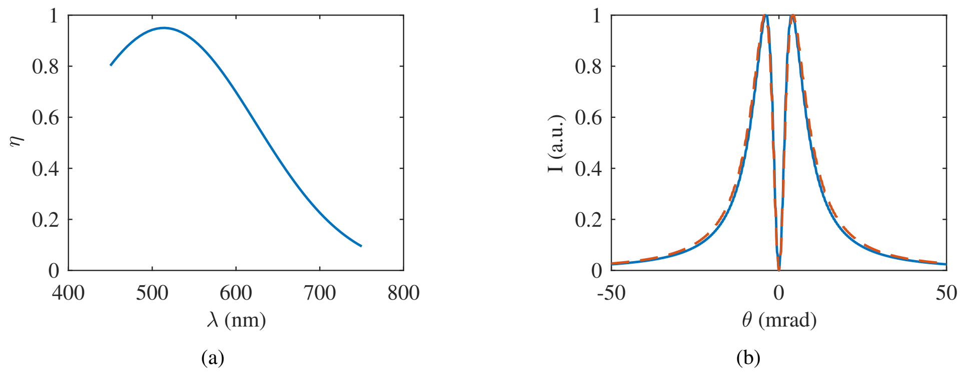

Figure 2: CCD Quantum Efficiency (η) as a function of the wavelength λ (a) and horizontal profile of the SPF OTR angular distribution for an energy of 123 MeV. The blue continuous line represents the monochromatic simulation, the red dashed line is the polychromatic one.

for an energy of 5 MeV, one solution could be f_1 equal to 20 mm, f_2 equal to 10 mm and L equal to 17 mm in order to have 430 pixels between the two maxima of the angular distribution. For an energy of 320 MeV, one could choose f_1 equal to 200 mm, f_2 equal to 20 mm and L equal to 120 mm in order to have 490 pixels between the two maxima of the angular distribution.

The DLL defined in the POP mode propagates only a particle at a time and a wavelength at time; in order to take into account the full optical spectrum, one can use the Zemax Programming Languages (ZPL) provided by the software and implement an appropriate routine. The ZPL macro sets a different wavelength for each simulation and performs a weighted sum of the simulations in order to take into account changes of quantum efficiency of the used CCD with respect to the wavelength (a typical CCD has its maximum efficiency around a wavelength of 550 nm as can be seen on Figure 2).

Typically the effects are mitigated by the CCD that acts in a similar way as a green filter: its quantum efficiency frequency dependence is high at the 550 nm wavelength and goes quickly down at the others frequencies. Hence, different CCDs will produce a different behaviors and they may require the use of an optical filter.

The ZPL macro approach can be used also for evaluating the spatial distribution of the beam and its beam divergence. The ZPL macro takes the output of a particle tracking code (GPT or Elegant) as the input information about the beam distribution: with this method, one can evaluate also the effects of the energy spread. This method has been experimentally validated with data taken from the SPARC_LAB high brightness electron Linac [6], that was analyzed in [15] (Fig. 3).

The beam has an energy of 123 MeV with an energy spread of 0.06%, the charge is 120 pC and the spot size is 278 µm and 115 µm in the horizontal and vertical plane respectively; the normalized emittance are 5 µm on the x and 3 µm on the y plane (beam divergence respectively 1.3 mrad and 1.2 mrad) while the bunch length is 1 ps. However, the bunch length information is not used yet and it will be implemented in the future development; for these values wavelengths of observation, the bunch length can be neglected (incoherent radiation).

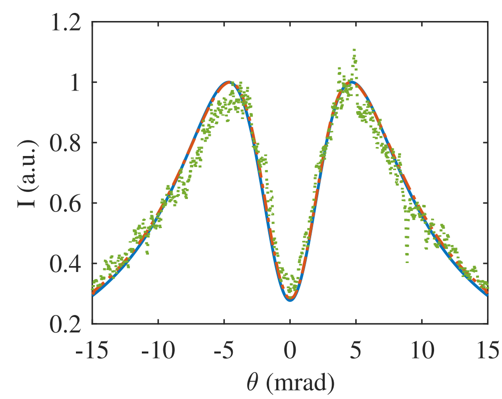

Figure 3: Horizontal profile of the beam angular distribution for an energy of 123 MeV and a divergence of 1.3 mrad: the blue continuous line represents the Zemax simulation, the red dotted line is the theory (Eq. 2) and the green dots represent the experimental data.

CONCLUSION

It has been shown a simulation model of the Far Field OTR of a typical beam: this model has been validated both with the theory and with the experimental data.

This model can take advantage of the results of particle tracking code like GPT or Elegant, in order to studies the OTR produced by beams with any phase-space distribution.

The ZPL macro method will be useful also to take into consideration the effects of an high energy spread on the OTR: this will help, for instance, for plasma accelerated beams [18].

Finally, in order to design the proper optics for a distributed energy beam, one must use a relay optics system: in this way, one can demagnify the angular distribution at low energies (i.e. 5 MeV), or magnify it at high energies (i.e. 300 MeV).

ISBN: 978-3-95450-184-7 doi:10.18429/JACoW-IPAC2018-WEPAL013

REFERENCES

[1] A. Bacci *et al.*, “Electron linac design to drive bright Compton back-scattering gamma-ray sources,” *Journal of Applied Physics*, vol. 113, no. 19, p. 194508, 2013.

[2] M. Marongiu *et al.*, “Thermal behavior of the optical transition radiation screens for the eli-np compton gamma source,” *Nuclear Instruments and Methods in Physics Research Section A*, 2016.

[3] D. Filippetto *et al.*, “Phase space analysis of velocity bunched beams,” *Physical Review Special Topics-Accelerators and Beams*, vol. 14, no. 9, p. 092804, 2011.

[4] A. Mostacci *et al.*, “Chromatic effects in quadrupole scan emittance measurements,” *Physical Review Special Topics-Accelerators and Beams*, vol. 15, no. 8, p. 082802, 2012.

[5] A. Cianchi *et al.*, “Six-dimensional measurements of trains of high brightness electron bunches,” *Physical Review Special Topics-Accelerators and Beams*, vol. 18, no. 8, p. 082804, 2015.

[6] M. Ferrario *et al.*, “Sparc_lab present and future,” *Nuclear Instruments and Methods in Physics Research Section B*, vol. 309, pp. 183–188, 2013.

[7] P. Antici *et al.*, “Laser-driven electron beamlines generated by coupling laser-plasma sources with conventional transport systems,” *Journal of Applied Physics*, vol. 112, no. 4, p. 044902, 2012.

[8] A. R. Rossi *et al.*, “The external-injection experiment at the sparc_lab facility,” *Nuclear Instruments and Methods in Physics Research Section A*, vol. 740, pp. 60–66, 2014.

[9] A. Giribono *et al.*, “6d phase space electron beam analysis and machine sensitivity studies for eli-np gbs,” *Nuclear Instruments and Methods in Physics Research Section A*, vol. 829, pp. 274–277, 2016.

[10] “Hamamatsu,” https://www.hamamatsu.com/sp/sys/en/manual/C11440-22CU_IM_En.pdf.

[11] M. Marongiu *et al.*, “Optical issues for the diagnostic stations for the eli-np compton gamma source,” in *8th Int. Particle Accelerator Conf.(IPAC’17), Copenhagen, Denmark*, 2017, pp. 238–241.

[12] F. Cioeta *et al.*, “Spot size measurements in the eli-np compton gamma source,” in *5th Int. Beam Instrumentation Conf.(IBIC’16), Barcelona, Spain*, 2017, pp. 533–536.

[13] V. Ginsburg *et al.*, “Radiation of a uniformly moving electron due to its transition from one medium into another,” *Zhurnal eksperimentalnoi i teoreticheskoi fiziki*, vol. 16, no. 1, pp. 15–28, 1946.

[14] M. Castellano *et al.*, “Analysis of optical transition radiation emitted by a 1 mev electron beam and its possible use as diagnostic tool,” *Nuclear Instruments and Methods in Physics Research Section A*, vol. 357, no. 2, pp. 231–237, 1995.

[15] M. Marongiu *et al.*, “Energy measurements by means of transition radiation in novel linacs,” *Nuclear Instruments and Methods in Physics Research Section A*, 2018, in press.

[16] “Zemax optic studios,” https://www.zemax.com/products/opticstudio.

[17] F. G. Bisesto *et al.*, “Zemax simulations describing collective effects in transition and diffraction radiation,” *Optics Express*, vol. 26, no. 4, p. 5075, 2018.

[18] M. Ferrario *et al.*, “Eupraxia@sparc_lab: design study towards a compact fel facility at lnf,” *Nuclear Instruments and Methods in Physics Research Section A*, 2018, in press.